Journal of Neural Engineering

PAPER

Electrochemical and biological characterization of thin-film platinum-iridium alloy electrode coatings: a chronic *in vivo* study

Ashley N Dalrymple[1], Mario Huynh[1], Bryony A Nayagam[1,2], Curtis D Lee[3], Greg R Weiland[3], Artin Petrossians[3], John J, Whalen III[3], James B Fallon[1,4] and Robert K Shepherd[1,4,5]

[1] Bionics Institute, St. Vincent's Hospital, Melbourne, VIC, Australia
[2] Department of Audiology and Speech Pathology, University of Melbourne, Melbourne, VIC, Australia
[3] Platinum Group Coatings, LLC, Pasadena, CA, United States of America
[4] Medical Bionics Department, University of Melbourne, Melbourne, VIC, Australia
[5] Author to whom any correspondence should be addressed.

E-mail: rshepherd@bionicsinstitute.org

Keywords: electrical stimulation, neural prosthesis, electrochemistry, platinum, electrodeposited Pt-Ir, tissue response, cochlear implants

RECEIVED
16 February 2020

REVISED
22 April 2020

ACCEPTED FOR PUBLICATION
14 May 2020

PUBLISHED
17 June 2020

Abstract

Objective. To evaluate the electrochemical properties, biological response, and surface characterization of an electrodeposited Platinum-Iridium (Pt-Ir) electrode coating on cochlear implants subjected to chronic stimulation *in vivo. Approach.* Electrochemical impedance spectroscopy (EIS), charge storage capacity (CSC), charge injection limit (CIL), and voltage transient (VT) impedance were measured bench-top before and after implant and *in vivo*. Coated Pt-Ir and uncoated Pt electrode arrays were implanted into cochlea of normal hearing rats and stimulated for ~4 h d, 5 d week^{-1} for 5 weeks at levels within the normal clinical range. Neural function was monitored using electrically-evoked auditory brainstem responses. After explant, the electrode surfaces were assessed, and cochleae examined histologically. *Main results.* When measured on bench-top before and after stimulation, Pt-Ir coated electrodes had significantly lower VT impedance ($p < 0.001$) and significantly higher CSC ($p < 0.001$) and CIL ($p < 0.001$) compared to uncoated Pt electrodes. *In vivo*, the CSC and CIL of Pt-Ir were significantly higher than Pt throughout the implantation period ($p = 0.047$ and $p < 0.001$, respectively); however, the VT impedance ($p = 0.3$) was not. There was no difference in foreign body response between material cohorts, although cochleae implanted with coated electrodes contained small deposits of Pt-Ir. There was no evidence of increased neural loss or loss of neural function in either group. Surface examination revealed no Pt corrosion on any electrodes. *Significance.* Electrodeposited Pt-Ir electrodes demonstrated significant improvements in electrochemical performance on the bench-top and *in vivo* compared to uncoated Pt. Neural function and tissue response to Pt-Ir electrodes were not different from uncoated Pt, despite small deposits of Pt-Ir in the tissue capsule. Electrodeposited Pt-Ir coatings offer promise as an improved electrode coating for active neural prostheses.

1. Introduction:

Cochlear implants provide severe-profoundly deaf individuals with important auditory cues required to understand human speech and appreciate environmental sounds [1]. These devices selectively stimulate primary auditory neurons (ANs) via a longitudinal array of platinum (Pt) electrodes located in the scala tympani [2, 3]. Electrical stimulation activates nearby ANs, providing a tonotopic sensation of sound to the user. Cochlear implants typically contain Pt electrodes, as Pt is both biocompatible [4, 5] and electrochemically stable under active conditions [6].

Although current cochlear implant systems are successful in improving the quality of life in people with a severe-profound hearing loss, users have reported difficulty in understanding speech in noisy environments and exhibit poor music perception [7, 8]. This is attributed, in part, to current spread resulting in the activation of a large number of ANs with a single electrode [9–11]. Improving the stimulation strategy, reducing the size of electrodes, and

increasing the number of electrodes along the cochlear array, may reduce the current spread to provide more accurate frequency discrimination to users by more precisely activating the target tissue [12, 13].

Reducing the size of the electrode increases the electrode impedance and charge density, as greater charge per unit area is required to activate ANs. Higher charge densities increase the risk of exceeding the water window for safe stimulation [6]. An option that could mitigate these risks and enable the use of more and/or smaller electrodes is the use of a high surface area conductive coating over the metal electrode surface. Conductive coatings can modify the performance of both: (i) recording electrodes by reducing both the impedance of the recording site and the level of thermal noise [14, 15]; and (ii) stimulating electrodes by reducing the impedance while increasing the charge storage capacity (CSC) and the charge injection limit (CIL) of the electrode [15–18].

A variety of approaches, including the application of conductive polymers [14–17, 19–22] or high surface area, low impedance metal coatings (including metals, such as iridium (Ir), with high oxidation states) using sputtering [23, 24], electrophoretic [25] or electrodeposition [26] techniques have been evaluated *in vitro* and *in vivo*. While many of these coatings provide significant improvement in the electrochemical performance of stimulating and recording electrodes *in vitro*, there are a number of significant challenges to be overcome before they can be considered suitable for clinical application [27, 28]. These challenges include evidence of delamination of the coating [17, 26, 29], and an increase in electrode impedance *in vivo* [15, 16, 30] attributed to the effects of the tissue encapsulation of the electrode dominating the impedance by reducing the exposed electrode surface area, thereby reducing the capacitance of the conductive coating [16].

Electrodeposited Pt-Ir is a coating that has been shown to lower impedance and increase the CSC by increasing the effective area of the electrode surface [31, 32]. It has been successfully coated on cochlear implant electrodes [32] and maintained an electrochemical advantage over uncoated Pt electrodes after an *in vitro* accelerated aging protocol [33]. Moreover, Pt-Ir coated micro-recording electrodes chronically implanted into the brain of rats over a period of 12 weeks displayed substantially lower impedance at 1 kHz and increased signal-to-noise ratio compared to uncoated electrodes [34]. This study also showed no significant difference in the immune response between Pt-Ir coated and uncoated electrodes.

High surface area Pt-Ir coatings have the potential to improve cochlear implant and other neural interfaces by reducing the electrode impedance while increasing both the CSC and CIL. Therefore, we evaluated the performance of electrodeposited Pt-Ir coatings on cochlear implant electrodes in a chronic active *in vivo* setting by comparing the electrochemical performance, electrode surface features, and the biological response of electrodeposited Pt-Ir coatings with conventional Pt electrodes.

2. Methods:

2.1. Experimental subjects

This study was performed using a total of 10 healthy young adult Sprague Dawley rats. The animals weighed 346 ± 18 g (mean ± standard deviation) at the time of surgery. The timeline for experiments performed in this study is illustrated in figure 1. All procedures were conducted with approval from the Bionics Institute Animal Research and Ethics Committee, and were performed in accordance with the Australian Code of Practice for the Care and Use of Animals for Scientific Purposes (8th Edition, 2013) and followed the principles of the US National Institutes of Health guidelines regarding the care and use of animals for experimental procedures.

2.2. Cochlear electrode array and electrodeposition of Pt-Ir

Cochlear implant electrode arrays were manufactured in-house (Bionics Institute, Melbourne, Australia) using the same biomaterials as used in clinical devices. Briefly, four Pt ring electrodes (E1 to E4; figure 1), each 0.3 mm in width, with an inter-electrode separation of 0.45 mm, were located near the tip of a medical grade silicone carrier [35]. The tip electrode had a diameter of 0.31 mm, tapering to 0.37 mm at the fourth electrode. Insulated Pt-Ir (90/10) wire (25 μm in diameter) connected each Pt ring to a percutaneous connector designed to be mounted on the animal's skull (figure 1). Each implant assembly was ultrasonically cleaned in a Pyroneg/distilled water solution (15 min), two rinses in distilled water (5 min each), 96% ethanol (10 min) followed by two additional two rinses in distilled water (5 min each). Six devices were shipped to Platinum Group Coatings LLC (Pasadena, CA, USA) for Pt-Ir coating.

High surface area Pt-Ir was electrodeposited onto the Pt surface of the electrodes from six cochlear arrays using previously described methods [31, 36]. A pre-implant image of the cochlear array implanted in PtIr03 is shown in figure 1(a). Small regions were devoid of Pt-Ir where the base metal was not coated. Uncoated regions are possibly due to non-conductive regions on the electrode surface which prevented the electrodeposition of Pt-Ir.

2.3. Bench-top electrochemical measurements

Before implantation and after removal of the cochlear arrays following the 5-week implantation program, a conventional 3 electrode setup was used for bench-top electrochemical measurements (figure 1(b)). These recordings consisted of the cochlear array containing the active electrodes (E1-E4), a Ag|AgCl reference electrode (Ionode, Australia), and a large Pt foil

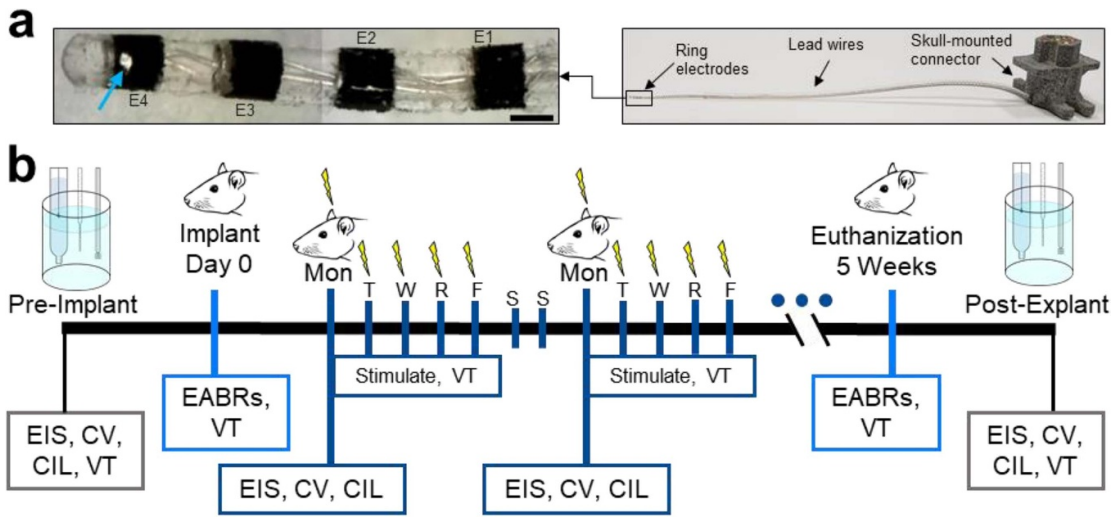

Figure 1. Study overview. (a) Coated cochlear electrode array (PtIr03) with four electrodes (E1-E4) and skull-mounted percutaneous connector. The arrow indicates a small region devoid of Pt-Ir coating pre-implant due to an absence of conductivity on that portion of the base metal. Scale bar = 0.3 mm. (b) Timeline for recordings and stimulation. A 3-electrode setup (illustrated) was used to record electrochemical impedance spectroscopy (EIS), cyclic voltammograms (CVs), charge injection limit (CIL) and voltage transient (VT) impedances prior to implantation and after explantation. Immediately after implant and on completion of the stimulation protocol, electrically-evoked auditory brainstem responses (EABRs) and VT impedances were recorded. Stimulation was delivered for 4 to 6 h every weekday (indicated by lightning bolts) for 5 weeks (repeated stimulation/recording in weeks 3–5 indicated by blue dots). Rat illustrations indicate *in vivo* recordings.

counter electrode (Ionode, Australia). All measurements were made in Dulbecco's phosphate-buffered saline (DPBS; ThermoFisher Scientific; Massachusetts, USA) at room temperature (~22 °C). Explanted arrays were rinsed with DPBS, and the electrode region of the array was left to soak overnight in DPBS to allow for equilibrium at the electrode-electrolyte interface and drying of the connector.

Electrochemical impedance spectroscopy (EIS) was performed using a potentiostat (Interface 1000E, Gamry Instruments, USA). The frequency values ranged from 100 000 to 1 Hz at 10 points/decade and an AC voltage of 50 mV rms. Cyclic voltammetry (CV) followed the EIS measurements and was also performed using the potentiostat. The electrode potential cycled between −0.6 and 0.8 V at a sweep rate of 150 mV s^{-1} for 10 cycles. To calculate the CSC, the average of cycles 2 through 10 were averaged, then the absolute value of the anodic and cathodic phases was integrated. This value was then divided by the geometric surface area of the electrode (which ranged from 0.29 to 0.35 mm^2) to produce the charge density for the CSC. Voltage transient (VT) waveforms were collected and used to compute the CIL and impedance of each electrode (USB-6353, National Instruments, USA). The CIL is the charge that can be delivered to produce a maximum cathodal voltage (E_{mc}) equal to the cathodal limit of the water window (−0.6 V) [6, 37]. The CIL was computed by analysing the voltage response to biphasic, cathodic-first current pulses with a pulse width of 100 μs and current amplitudes from 50 μA to 2 mA in steps of 50 μA. The E_{mc} of the response was determined by subtracting the access voltage (V_a) from the maximum negative potential. The CIL was computed using the current value just below the level that caused the E_{mc} to exceed the cathodal polarization limit of −0.6 V, up to a maximum of 2 mA. The VT impedance was computed by recording the peak voltage in response to current injection during the first phase of a single biphasic, cathodic-first current pulse with a pulse width of 100 μs and amplitude of 100 μA. The lowest possible impedance value that could be recorded was equal to 1.23 kΩ due to the internal resistance of the stimulating device.

2.4. Surgical procedure

Animals were randomly selected to receive either a Pt electrode array or an electrode array where the Pt electrodes were electrodeposited with a coating of Pt-Ir. Each animal was anesthetized with isoflurane 2% to 3% in oxygen (1 l min^{-1}). Surgery was performed under sterile conditions with the animal's temperature monitored using a rectal probe and maintained at 37 °C using a heating pad. Following administration of analgesics (0.3 ml of lignocaine hydrochloride, topical; Troy Laboratories, Australia; and carprofen, 5 mg kg^{-1}, subcutaneous; Norbrook, Australia), the nasal region of the skull was exposed, and the percutaneous connector was mounted onto the skull using stainless steel screws and dental cement (Paladur, Germany). A left postauricular approach was used to expose the auditory bulla and the round window of the cochlea. After cauterizing the stapedial artery [35], the round window membrane was incised via a small cochleostomy in the lower basal turn, and the electrode array was inserted ~5 mm into the scala tympani. The round

window was sealed with muscle followed by fascia, and the lead-wire proximal to the electrode array was fixed inside the bulla with Kwik-Cast elastomer (WPI Inc. USA) and carboxylate cement (Durelon, Germany). The distal end of the lead-wire was tunnelled subcutaneously to the percutaneous connector. The wounds were sutured in two layers with Visorb 3/0 (CP Medical, USA). Each animal received Hartmann's solution (10 ml kg^{-1}, subcutaneous) and the analgesic Temgesic (0.03 mg kg^{-1}, subcutaneous; Reckitt-Benckiser, UK) immediately after surgery to aid with recovery. No surgery was performed on the right cochlea.

2.5. EABRs and impedances

Electrically-evoked auditory brainstem responses (EABRs) were recorded to confirm array placement in the cochlea and to monitor neural function. EABRs were recorded immediately following implant surgery and on completion of the 5-week stimulation protocol. All recordings were performed with the animal under general anesthesia (isoflurane 1.5% to 2.5% in oxygen, 1 l min^{-1}). Briefly, biphasic current pulses (300 μs per phase; 50 μs interphase gap) were used to stimulate the electrode configuration used in the 5-week stimulation protocol. Scalp recorded responses from subcutaneous needle electrodes (vertex positive; neck negative; thorax ground) were recorded to a computer and averaged over 100 trials [38]. Recordings were made at intensity intervals presented randomly from below threshold to a maximum of 260 Current Level (CL; where the current in $\mu A = 17.5 \times 100^{CL/255}$).

2.6. Chronic stimulation program

Rats were given several days to recover from surgery prior to commencing chronic stimulation, which began on the Monday following the surgery (figure 1(b)). The rats were stimulated for 4 to 6 h per day for 5 d per week using a custom-built stimulator [39]. Stimulation was delivered using charge-balanced biphasic current pulses at 300 μs $phase^{-1}$ at 100 pulses per second (pps) up to 200 μA in a tripolar configuration [38]. Charge balance was achieved using electrode shorting and capacitive coupling [40]. In this configuration, a cathodic-first current pulse was delivered to the electrode at the centre of the tripole, with the two adjacent electrodes connected together to provide a return path. All currents were then reversed in the second phase of the pulse. The fourth electrode on the array (E1) was not stimulated and served as a control. A maximum current amplitude of 200 μA was presented to the centre electrode (E3) of the tripole delivering a charge density of 19.3 $\mu C\ cm^{-2}\ phase^{-1}$ while the flanker electrodes (E2 and E4) received approximately half this charge density.

A tripolar configuration was chosen since it recruits less auditory neurons per charge/phase than conventional monopolar stimulation [41]; because this evokes a quieter percept it is more accepted by the animals. If the animal exhibited an adverse response to a stimulus amplitude of 200 μA the level was reduced to 100 μA (n = 1 animal; table 1). Finally, if stimulation using the tripolar configuration was not possible, for example due to high electrode impedance (>20 kΩ) or lead wire breakage, a bipolar configuration was used whereby one electrode served as the active electrode and another as the return electrode (n = 2 animals; table 1).

2.7. In vivo electrochemical measurements

At the beginning of each week up to 5 weeks post-implantation, EIS, CV, and CIL were recorded *in vivo* (figure 1(b)). Since a 3-electrode recording configuration was not feasible *in vivo*, the electrochemical measurements were made using the same recording equipment as in the 3-electrode set-up, but with the tripolar or bipolar configuration that was used for delivering stimulation. The frequency values in the EIS ranged from 100 000 to 100 Hz at 10 points/decade and an AC voltage of 50 mV rms. The low frequency value was increased from 1 to 100 Hz compared to the bench-top recordings to avoid the possibility of DC-induced tissue damage. EIS measurements were followed by CV, where the electrode potential cycled between − 0.6 and 0.8 V at a sweep rate of 150 mV s^{-1} for 10 cycles. The CIL for the tripolar electrode configuration was measured using the same technique as the bench-top measurement. VT impedances for each electrode were collected before and after stimulation each weekday. If any electrodes had a VT impedance greater than 20 kΩ, that electrode was considered open circuit and prompted a change in the electrode configuration from tripolar to bipolar (table 1) and were excluded from electrochemical analysis beyond that time point.

2.8. Histology

On completion of the stimulation protocol all animals were euthanized with an overdose of sodium pentobarbitone (Intraperitoneal; Virbac, Australia) and systemically perfused with heparinized normal saline at 37 °C followed by 10% neutral buffered formalin (NBF) at 4 °C. The electrode array was removed for examination under a scanning electron microscope (SEM; see below) and the cochleae were post-fixed for 1 h in NBF and then washed three times in 0.1 M phosphate buffered saline at room temperature. Cochleae were decalcified in 10% (wt vol)$^{-1}$ ethylene diamine tetra-acetic acid, cryoprotected with 15%, then 30% sucrose overnight, before being infiltrated and embedded in Tissue-Tek O.C.T. cryosectioning compound (Sakura, Japan), snap frozen and stored at −80 °C. Cochleae were sectioned at 12 μm using a CM 1850 cryostat (Leica, Germany) at −22 °C and sections were mounted onto Superfrost-Plus slides (Menzel-Gläser, Germany). A representative

Table 1. Summary of animal groups and stimulation parameters. Changes in stimulation configuration and parameters during the implant period are separated by a semi-colon. Inclusion for analysis was based on electrical integrity of the array and confirmation that the array was located in the cochlea using histology and electrically-evoked auditory brainstem responses (EABRs). Group data are represented by mean (± standard deviation). TP = tripolar; BP = bipolar.

Animal ID	Implant duration (days)	Hours Stimulated	Days Stimulated	Stimulation Configuration	Current Amplitude (mA)	Charge Density (μC cm^{-2} phase)
Pt01	34	81.1	17	TP E3	0.2	19.3
Pt02	33	100.3	21	TP E3	0.2	19.3
Pt03	34	100.7	22	TP E3	0.2	19.3
Pt04	32	100	21	TP E3	0.2	19.3
Pt05	35	102.4	23	TP E3	0.2	19.3
PtIr01	35	92.5	23	TP E3	0.2	19.3
PtIr02	35	92.8	22	BP E1-E2	0.1	9.1
PtIr03	35	26.7; 65.1	7; 14	TP E3; BP E3-E4	0.2	19.3
PtIr04	35	103.2	23	TP E3	0.2	19.3
PtIr05	35	105.2	23	TP E3	0.2	19.3
Pt	33.6 ± 1.1	96.9 ± 8.9	20.8 ± 2.3	TP E3	0.2 ± 0	19.3 ± 0
Pt-Ir	35 ± 0	97.1 ± 6.5	22.4 ± 0.9	TP and BP	0.18 ± 0.04	17.3 ± 4.6

histological series were stained with Mayer's haemotoxylin and Putt's eosin (H&E) for examination.

The extent of auditory nerve survival (measured as AN density) and the foreign body tissue response within the scala tympani of the upper basal (UB) turn close to the stimulating electrodes were quantified for each animal. The AN density was determined by digitally imaging Rosenthal's canal at ×20 magnification using a Zeiss AxioLab microscope. Using Image J software (Image J [42];), ANs were identified within Rosenthal's canal and counted within the UB turn of the cochlea by a single observer blinded to the experimental cohorts. The area of Rosenthal's canal was then measured and the AN density determined [38]. The AN density was averaged from 4 sections spaced at least 72 μm apart to ensure that no AN was counted twice.

The foreign body response in the cochlea was measured in H&E stained sections at four locations along the electrode array in the UB turn. An image of the scala tympani at ×10 was captured and its area measured. The 'Triangle' algorithm in Image J was used to threshold the image in order to quantify the tissue response. The area of scala tympani, excluding the area of the electrode array, was measured and the proportion of the scala tympani occupied by the tissue response calculated [43]. The tissue capsule was also qualitatively examined for evidence of particulate material within the tissue capsule and H&E sections were used to examine the response of macrophages to electrodeposited Pt-Ir. Finally, a number of unstained histological sections from cochleae exhibiting particulate material were examined under the SEM and energy dispersive x-ray spectroscopy (EDS) was used to identify the material (see below).

2.9. Scanning electron microscopy

2.9.1. Electrode surface characterization

Following removal from the cochlea, each electrode array was rinsed in distilled water then stored in 70% ethanol before being examined for evidence of surface coating delamination and Pt corrosion using a FEI QUANTA 200 SEM. All 4 electrodes on each electrode array were photographed at low (×600) and medium (×2000) magnification. A region of each electrode surface was then randomly selected and photographed at ×4000 by a microscopist naïve to the experiment. The surface condition of each electrode was evaluated by an investigator blinded to the experimental groups. Morphological features and grayscale discolouration that could indicate mechanical damage, pitting corrosion, intergranular corrosion and surface deposits were evaluated and the severity of base metal Pt corrosion was graded from 0 (no corrosion) to 5 (severe and extensive corrosion) [38]. The coverage of Pt-Ir was also visually assessed.

2.9.2. Particulate matter in tissue

Representative unstained cochlear sections were examined under the SEM to identify particulate matter observed within the fibrous tissue capsule of some cochleae. Specific sites associated with the tissue capsule were selected for elemental analysis using an INCA X-Act SDD EDS system with an Oxford Aztec Microanalysis System (3.1) [38]. Regions of the fibrous tissue capsule containing the particulate material were compared with regions only containing fibrous tissue.

2.10. Statistical analysis

For all comparisons, Shapiro-Wilk was used to test normality and Brown-Forsythe tested the homogeneity of variance. $p \leq 0.05$ was used to indicate significance for all tests. Data are presented as median and quartiles unless otherwise stated.

Electrochemical measurements including EIS, CSC, and VT impedance before implant and after explant (bench-top 3 electrode recording) and at week 1 and week 5 (*in vivo* tripolar recording), as well as EABR thresholds after surgery and at termination were compared using two-way repeated measures

analysis of variance (ANOVA). CIL *in vivo* was compared between materials using a linear mixed model to include all 5 weeks of recordings. CSC, CIL and VT impedance were compared across different stimulation charge densities using a one-way ANOVA. All pairwise comparisons were performed using the Holm-Sidak method if the ANOVA was significant. The area of the scala tympani occupied by fibrous tissue was compared for the two material groups using the Mann-Whitney test. AN density was compared for the two material groups using the Student's t-test. Correlations between the stimulation charge density and the coating coverage, CSC, CIL, and VT impedance were made using the Pearson Product-Moment correlation.

3. Results:

The present results were based on data from five rats implanted with Pt and five rats implanted with Pt-Ir coated electrode arrays (table 1). The rats were implanted for 32 to 35 d and received between 81.1 and 105.2 h of stimulation. All rats from the Pt group and three out of five rats from the Pt-Ir group were stimulated using a tripolar configuration at 200 μA for the entire implant duration. One rat from the Pt-Ir group was stimulated using a bipolar configuration at 100 μA and one rat received tripolar stimulation for the first week, followed by bipolar stimulation for the remaining implant duration; both configurations with a stimulation amplitude of 200 μA. Note that data from the Pt control cohort were also used in [44].

3.1. Bench-top electrochemical measurements pre- and post-stimulation

Bench-top electrochemical measurements using a 3-electrode setup were performed before implantation of the arrays and after they were explanted from the cochlea. Pt-Ir coated electrodes had significantly lower impedance than Pt at 1 Hz, 1 kHz, and 100 kHz before implantation and following their removal from the cochleae ($p < 0.001$; figure 2(a)). The impedance magnitudes at 1 Hz for both Pt and Pt-Ir did not change significantly over time; however, the impedance magnitudes of both materials significantly differed with time at 1 kHz ($p < 0.001$) and at 100 kHz ($p < 0.001$). The phase of the Pt-Ir coated electrodes after explantation approached zero at a lower frequency than they did pre-implantation (figure 2(b)). The CSC of Pt-Ir remained significantly greater than the CSC for Pt after explant ($p < 0.001$), despite significantly decreasing from the pre-implant value ($p < 0.001$; figures 2(c)–(d). Pt-Ir coated electrodes had a significantly higher CIL before implantation ($p < 0.001$) and after explantation ($p < 0.001$) compared to Pt (figure 2(e)). Both Pt and Pt-Ir electrodes had a significant increase in the CIL after explantation compared to before implantation ($p < 0.001$). The VT impedances of Pt-Ir coated electrodes were significantly lower than Pt electrodes both before implantation and after explantation ($p < 0.001$; figure 2(f)). The VT impedance of both Pt and Pt-Ir electrodes measured after explantation did not significantly differ from their pre-implantation values. Overall, Pt-Ir coated electrodes exhibited significant electrochemical advantage over Pt electrodes both before implantation and following explantation.

3.2. Electrically-evoked responses

EABRs were recorded immediately after surgery and at the completion of the 5-week stimulation protocol and were used to verify that the arrays were within the cochlea as well as to monitor the status of the ANs (figure 3). The EABR threshold for Pt and Pt-Ir coated electrodes was not significantly different, nor did thresholds differ significantly over time (Mean endpoint thresholds: $\text{Thresh}_{\text{Pt}} = 179 \pm 19$ CL; $\text{Thresh}_{\text{PtIr}} = 167 \pm 40$ CL).

3.3. Electrochemical performance during chronic implantation and electrical stimulation

Since two of the five animals in the Pt-Ir group received bipolar rather than tripolar stimulation (table 1), tripolar electrochemical recordings were not collected at all time points during the implant period. If the electrochemical data for bipolar versus tripolar Pt-Ir electrodes were not statistically different at *in vivo* week 1, indicated by an independent samples t-test, then the data were grouped together for statistical analyses.

The magnitude of the EIS impedance at 100 Hz during the first week was significantly lower for Pt-Ir coated versus Pt electrodes ($p = 0.006$; figure 4(a)). At 5 weeks post-implantation there was no significant difference between Pt-Ir and Pt electrodes at 100 Hz. Differences in the impedance magnitudes at other frequencies were not compared statistically between the two electrode surfaces because there were significant differences between the values recorded using tripolar versus bipolar configurations for Pt-Ir electrodes. Overall, the CSC of Pt-Ir coated electrodes was significantly greater than Pt electrodes ($p = 0.047$) and did not differ significantly between week 1 and week 5 (figures 4(c)–(d), although there were some large individual differences in CSC over the implant period among both Pt-Ir and Pt electrodes (figure 4(e)).

The CIL of Pt-Ir coated electrodes was significantly higher than Pt electrodes as measured across all 5 weeks *in vivo* ($p < 0.001$; figure 5(a); linear mixed model statistics). Individually, three of the five coated electrode arrays maintained a high CIL; however, the CIL of two arrays decreased to values close to those of Pt (PtIr01, 02; figure 5(c)). In addition, one Pt CIL measurement during the first week was 13× higher than the next highest Pt CIL value for any week (Pt05). VT impedances

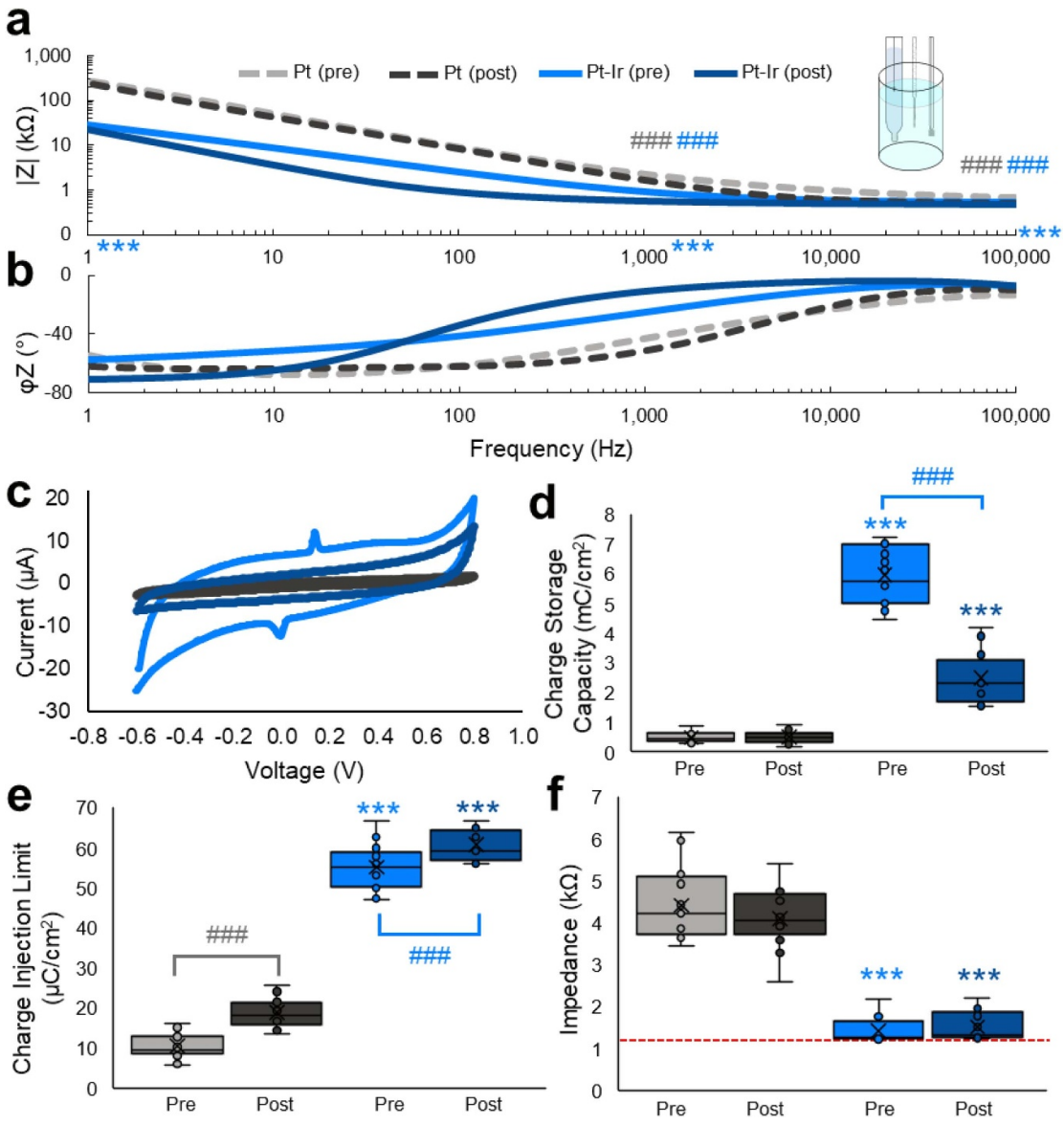

Figure 2. *Bench-top* electrochemical measurements recorded using a 3-electrode setup before implantation (pre) and after explantation (post). (a) Mean impedance (Z) magnitude from electrochemical impedance spectroscopy (EIS) for all electrodes of each material. (b) Mean impedance phase from EIS for all electrodes of each material. Pt data are dashed lines; Pt-Ir data are solid lines. (c) Representative cyclic voltammograms (CV) for each material. (d) Median, interquartile range and 95% confidence limits of the total charge storage capacity (CSC) calculated from the CV curves for each material. (e) Median, interquartile range, and 95% confidence limits of the charge injection limit (CIL) for each material. (f) Median, interquartile range, and 95% confidence limits for of the voltage transient (VT) impedance for each coating material. The horizontal red dashed line at 1.23 kΩ represents the lowest possible impedance of the recording device. In box and whiskers plots: × = mean, ◯ = raw data points. $^{*}p \leq 0.05$; $^{**}p \leq 0.01$; $^{***}p \leq 0.001$; #$p \leq 0.05$; ##$p \leq 0.01$; ###$p \leq 0.001$. * symbol denotes comparisons between materials at a single timepoint; # symbol denotes comparisons of the same material over time.

recorded from Pt-Ir electrodes immediately after surgery were significantly lower that Pt electrodes ($p < 0.001$; figure 5(b)); however, the VT impedance of the coated electrodes increased significantly during the implant period ($p < 0.001$) and were not significantly different from Pt electrodes following 5 weeks of implantation ($p = 0.3$). The majority of change in VT impedance of coated electrodes occurred within the first 7 d of implantation (figure 5(d)).

3.4. Cochlear histopathology

3.4.1. Tissue response

There was no evidence of electrode insertion trauma in the UB turn of any implanted cochlea. Therefore, any tissue reaction at this site was evoked by the biomaterials associated with the electrode array and/or the electrical stimulation, i.e. the tissue response was not masked by insertion trauma. Representative examples of the tissue response for both electrode materials are illustrated in figures 6 (a)–(b). This typically took the form of a thin, mature tissue capsule surrounding the electrode array, with loose mature fibrous tissue occupying the remainder of the scala tympani. The area of the scala tympani occupied by fibrous tissue did not significantly differ between Pt (10.2 ± 8.7%) and Pt-Ir electrodes (16.4 ± 22.7%; $p = 1.0$) (figure 6(c)). However, one implant array (PtIr02) had a much greater tissue response compared

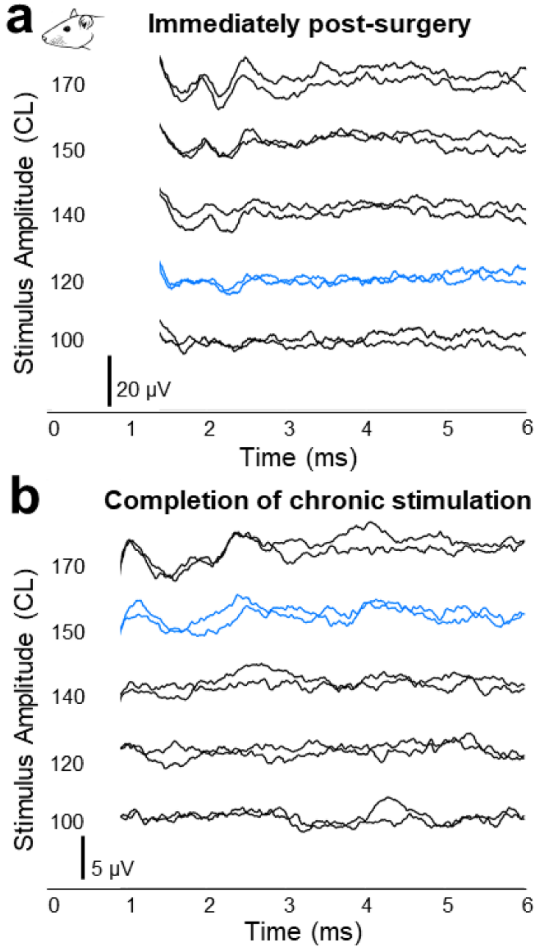

Figure 3. Representative electrically-evoked auditory brainstem responses (EABRs) recorded from PtIr01 (a) immediately after surgery and (b) at the completion of the 5-week stimulation protocol. The stimulation artefact has been removed. The EABR trace corresponding to the threshold current level (CL) is indicated in blue.

to the other arrays in the Pt-Ir cohort. This array also demonstrated the largest VT impedance *in vivo* (figure 5(d)). There was a strong correlation between the tissue response and the VT impedance at 5 weeks for Pt-Ir coated electrodes ($R^2 = 0.93$) but not for Pt electrodes ($R^2 = 0.03$). This correlation was largely affected by PtIr02, which had the greatest tissue response and VT impedance of all electrode arrays.

3.4.2. Auditory neuron survival

Representative micrographs of Rosenthal's canal illustrating ANs adjacent to Pt-Ir and Pt electrodes are illustrated in figures 6 (d)–(e). There was no significant difference in AN density between animals stimulated using Pt electrodes versus Pt-Ir electrodes ($p = 0.088$; figure 6(f)).

3.5. Electrode coating properties

3.5.1. Surface characterization of the electrodes

The surface of each electrode was graded by a blinded observer for corrosion or other features of mechanical damage of the underlying Pt. Here, corrosion was defined as a visible appearance of irregular surface roughness or variations in conductivity evidenced by differences in image grayscale intensity. No electrodes used in the present study exhibited evidence of corrosion or degradation of the underlying Pt. Some explanted electrodes had small amounts of tissue or other organic material (e.g. protein) on the surface (figures 7(a)–(c). The majority of Pt-Ir coated electrodes contained small areas devoid of the Pt-Ir coating (e.g. ×; figure 7(d)). Post-implantation quantification of the coated regions of the electrodes that were imaged at x 4000 indicated that one electrode was completely coated, 13 electrodes had 90% or more of the surface area coated, five electrodes had ∼80% of the electrode coated, and one electrode had approximately half its area coated (figure 7(e)). A similar analysis was not done prior to implantation for comparison, although qualitative light microscope imaging of the Pt-Ir coated electrode arrays prior to implantation revealed that some electrodes did not receive complete coating coverage (figure 1(a)). The presence of regions devoid of Pt-Ir on the coated samples was independent of whether or not the electrode had been stimulated ($R^2 = 0.11$). Additionally, there was no relationship between the coating coverage and the electrochemical performance of the electrodes after explant ($R^2 < 0.01$ for all measures).

3.5.2. Relationship with electrochemical measurements

The effect of the degree of stimulation, measured as charge density, on the electrochemical characteristics of the electrodes recorded using the 3 electrode bench-top set-up after the 5-week stimulation protocol was determined. The CSC of Pt electrodes differed significantly between unstimulated and centre electrodes ($p = 0.049$) but did not significantly differ for any of the Pt-Ir coated electrodes ($p = 0.873$; figure 7(f)). The CIL of Pt-Ir coated electrodes at the centre of the tripole (i.e. highest charge density) was significantly greater than the CIL of unstimulated electrodes ($p = 0.043$), with no difference in the CIL for Pt electrodes ($p = 0.167$; figure 7(g)). The VT impedance of flanking Pt electrodes was significantly lower than the VT impedance of unstimulated Pt electrodes ($p = 0.018$). Additionally, both Pt and Pt-Ir coated centre electrodes had a significantly lower VT impedance than unstimulated electrodes (Pt: $p = 0.006$; Pt-Ir: $p = 0.011$; figure 7(h)).

3.5.3. Particulate matter in tissue

Particulate matter of a metallic nature was observed in the tissue capsule of the stimulated cochleae of all animals with Pt-Ir coated electrodes. A representative example is illustrated in figure 8. EDS recordings under SEM confirmed the presence of Pt and Ir in the selected regions of the fibrous tissue containing the particulate matter and the absence of Pt and Ir in regions not containing the particulate matter (data not illustrated).

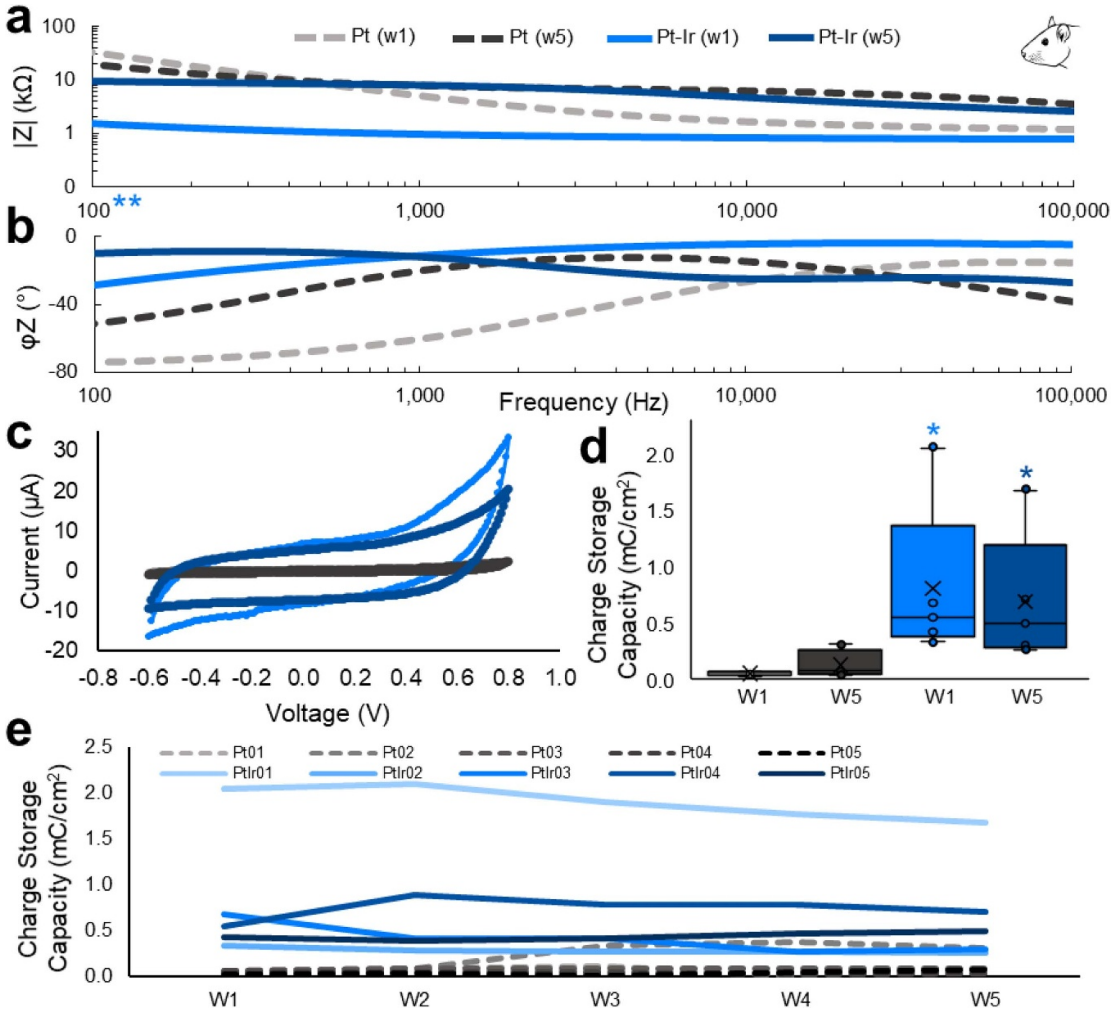

Figure 4. Weekly (w) electrochemical measurements recorded *in vivo*. (a) Representative magnitude of the impedance (Z) from electrochemical impedance spectroscopy (EIS). (b) Representative phase of the impedance from EIS. Pt data are dashed lines; Pt-Ir data are solid lines. (c) Same representative cyclic voltammograms (CV). (Representative data from Pt05, PtIr01). (d) Median, interquartile range and 95% confidence limits of for the total charge storage capacity (CSC) calculated from the area of the CV curves. (e) CSC for each animal throughout the implant duration. In box and whiskers plots: × = mean, ◯ = raw data points. $^{*}p \leq 0.05$; $^{**}p \leq 0.01$.

4. Discussion:

High surface area Pt-Ir was electrodeposited onto Pt cochlear electrodes, chronically implanted into rat cochleae and electrically stimulated at levels typically used clinically. The Pt-Ir coated electrodes were compared to conventional Pt electrodes using bench-top and *in vivo* electrochemical recordings. Tissue response, neural survival, and an evaluation of the electrode surface were undertaken to assess the biological response to chronic stimulation. The high surface area Pt-Ir coating displayed a significantly higher CSC and CIL and significantly lower impedance compared to Pt electrodes in bench-top recordings taken before and on completion of the implant period. *In vivo* electrochemical measurements of CSC and CIL for Pt-Ir electrodes made over the implantation period were significantly higher than Pt electrodes; however, VT impedance values were no longer significantly different from Pt electrodes by the fifth week of implantation. Histologically, Pt-Ir electrodes evoked a similar tissue response to that of Pt electrodes. There was no evidence of neural loss or loss of neural function associated with this coating; however, small amounts of particulate Pt-Ir were present in histological sections. This is the first *in vivo* evaluation of this coating under conditions of chronic electrical stimulation and serves as a pre-clinical assessment for future applications in neural prostheses.

4.1. Electrochemical performance of Pt-Ir electrodes:

In vivo, CIL and CSC remained significantly higher for Pt-Ir coated electrodes; however, VT impedance, which was significantly lower for Pt-Ir coated electrodes immediately following implantation, was no longer statistically different from Pt electrodes by the end of the implantation most likely due to an increase in tissue resistance surrounding the electrodes for both the coated and uncoated electrode arrays.

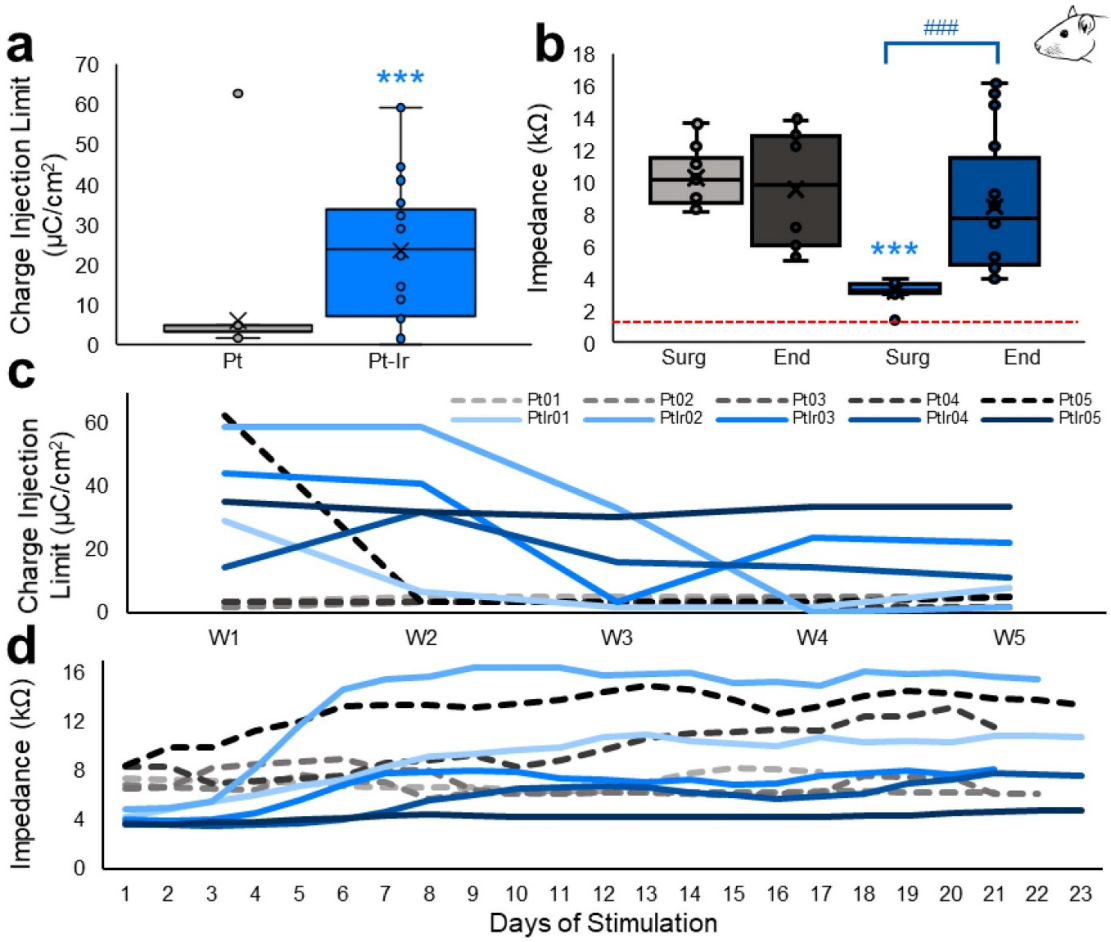

Figure 5. Electrochemical measurements recorded *in vivo*. (a) Median, interquartile range, and 95% confidence limits of the charge injection limit (CIL) calculated from the VT at all 5 weeks combined. (b) Median, interquartile range, and 95% confidence limits for the voltage transient (VT) impedances immediately after surgery (Surg) and on completion of the stimulation protocol (End). The horizontal red dashed line at 1.23 kΩ represents the lowest possible impedance of the recording device. (c) Weekly CIL for each animal throughout the implant duration. (d) Daily VT impedance for each animal after stimulation throughout the implantation period, smoothed using a moving average filter. Pt data are dashed lines; Pt-Ir data are solid lines. In box and whiskers plots: × = mean, ◯ = raw data points. ***$p \leq 0.001$; ###$p \leq 0.001$. * symbol denotes comparisons between materials at a single timepoint; # symbol denotes comparisons of the same material over time.

The increase in VT impedance for cochlear implant electrodes after implantation is well documented [45, 46] and consists of a gradual increase in access resistance which is associated with the formation of a tissue capsule around the electrode array, and a polarization impedance which increases in the absence of stimulation but decreases following stimulation. Novel high surface area/low impedance coatings generally have lower polarization impedance but similar access resistance compared to uncoated controls [32]. Therefore, when testing novel coatings *in vivo*, it is common for the access resistance (correlated with the extent of tissue response in the region of the electrodes) to increase for both novel and traditional electrodes and eliminate the statistical difference in the VT impedance (the access resistance plus the polarization impedance), while the polarization impedance of the novel electrode remains significantly lower than the uncoated electrode [30]. When these electrodes are removed from the tissue and measured in a low resistance solution (such as saline), the access resistance decreases due to the absence of a tissue capsule.

The electrodes in the current study followed this pattern and placing the array in saline (DPBS) following its removal from the cochlea significantly reduced the VT impedance to its pre-implant level. These findings suggest that while the polarization impedance of the Pt-Ir electrodes remained low during implantation period, the access resistance increased likely due to tissue encapsulation for both the coated and uncoated electrodes. Because the access resistance was large compared to the polarization impedance, it dominated the VT impedance and eliminated the significant difference present at the beginning of the study and on the bench top before and after implantation. The influence of the cellular response around the implanted electrode has also been described for chronically implanted microelectrodes monitored using EIS [16, 47].

Investigators examining the electrochemical performance of conductive polymer coated electrodes

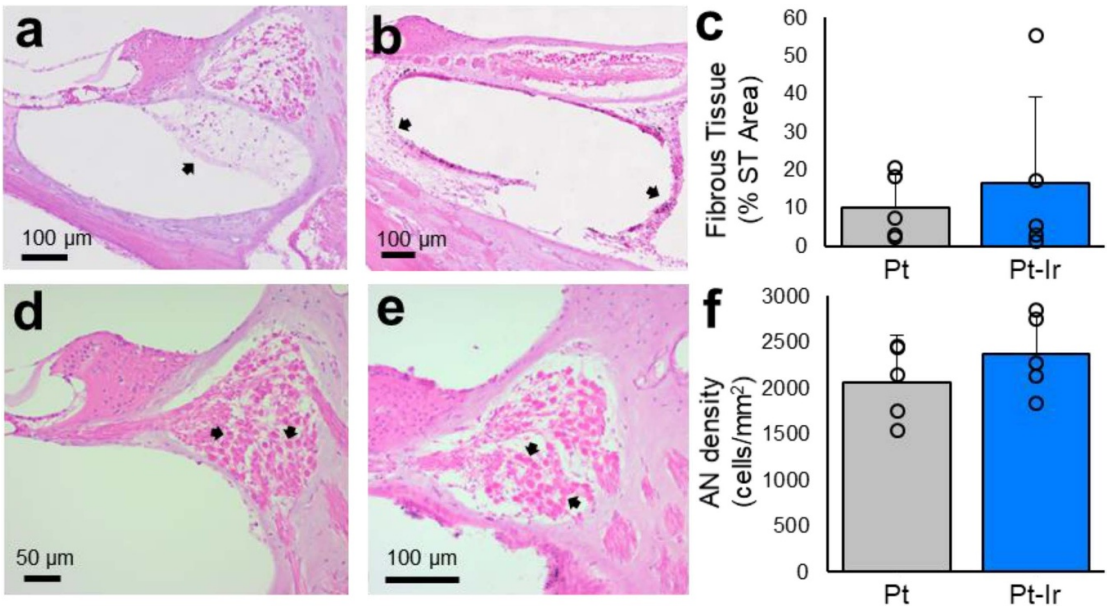

Figure 6. Tissue response to chronic stimulation. Representative tissue response in the upper basal turn of a cochlea stimulated using (a) uncoated Pt electrodes and (b) Pt-Ir coated electrodes. The tissue capsule is indicated with arrowheads. (c) Quantification of area of scala tympani (ST) occupied by fibrous tissue for all stimulated cochleae in each material cohort (mean ± standard deviation). Representative micrograph of Rosenthal's canal containing auditory neurons (ANs; e.g. arrows) from a rat with (d) uncoated Pt electrodes and (e) Pt-Ir coated electrodes. (f) Quantification of AN density for all stimulated cochleae in each cohort (mean ± standard deviation).

in vivo have also reported findings consistent with the present results, including an increase in electrode impedance while maintaining a high CSC compared with uncoated electrodes [14–16, 48]. Alba and colleagues [16] considered that these *in vivo* changes were a result of a reduction in surface capacitance of the electrode due to protein and cellular processes encapsulating and interpenetrating the porous coating.

We observed that the electrochemical performance of both Pt and Pt-Ir electrodes measured benchtop on completion of the implantation period was dependent on the stimulation history of the electrode. Electrodes with a high charge density exhibited favorable electrochemical measures compared to unstimulated electrodes including increased CSC (Pt), increased CIL (Pt-Ir), and decreased impedance (Pt and Pt-Ir). Since there was no evidence of corrosion determined using SEM, it is not certain why the stimulated electrodes had more favorable measures; however, an increase in CIL and CSC and decrease in impedance has been shown to occur as a result of cycling current through electrodes (either as a bi-product of stimulation [49] or deliberate 'rejuvenation' [34]). Pt [50] and especially Ir [51] have multiple oxidative states that become activated by cycling through positive and negative potentials *in vitro* [52]. Lower impedance, higher CSC, and improved signal-to-noise ratio has also been reported after stimulating Ir microelectrodes [53]. The electrodes were stimulated for 20–30 h per week, whereas they were cycled during CV measurements for only few minutes each week, using the same configuration. Both processes maintained a potential within the water window; therefore, it is reasonable to conclude that stimulation may contributed more to the change in impedance, and CIL values compared to CV measurements.

Two rats in the Pt-Ir cohort were stimulated with a bipolar instead of a tripolar configuration. We speculate that the loss of some electrodes on the Pt-Ir arrays was due to the additional handling and manipulation of these relatively delicate arrays during coating and shipping. We have reported a similar finding using an alternative coating [44], and are therefore confident that this effect is not related to the application of Pt-Ir *per se*.

4.2. The biological response of the cochlea to Pt-Ir electrodes

Both Pt-Ir and Pt electrodes evoked a mild foreign body response that, after 5 weeks of implantation, typically consisted of a thin, mature fibrous tissue capsule. Although a foreign body response may have contributed to the partial reduction in electrochemical performance of the Pt-Ir coating *in vivo*, the extent of the tissue response observed in the Pt-Ir implanted cochleae was similar to that associated with Pt electrodes. This finding, using macroelectrodes implanted in the cochlea, are consistent with those of Cassar *et al* [34], who reported no significant difference in the immune response between Pt-Ir coated and uncoated micro-electrodes passively implanted in the brain, nor did they report evidence of Pt-Ir coating removal during the implant period.

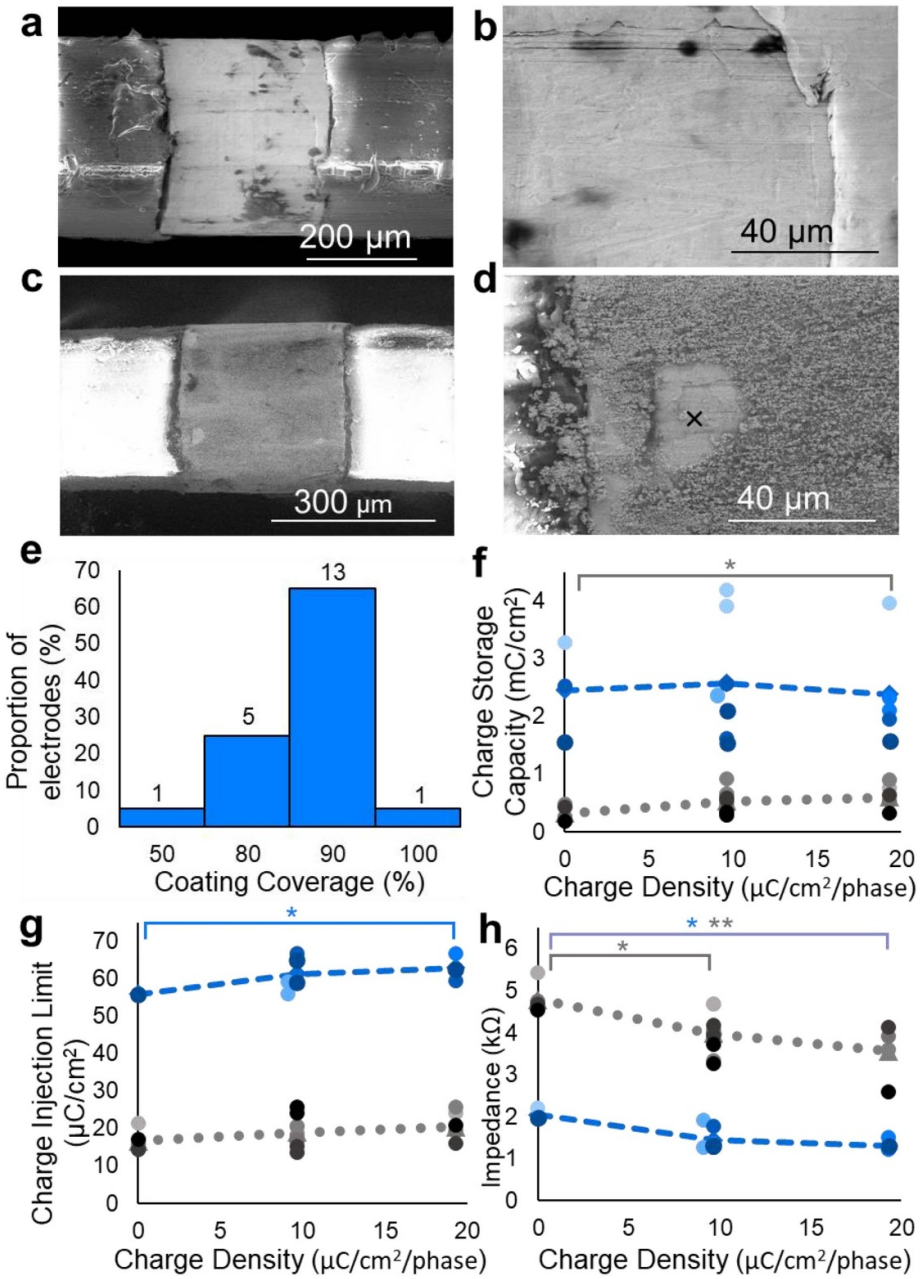

Figure 7. Effects of stimulation level on electrode surface characteristics and electrochemical performance examined after explantation. (a) Low magnification Pt electrode with some tissue remnants. (b) High magnification Pt electrode showing manufacturing marks but no evidence of surface corrosion. (c) Low magnification Pt-Ir coated electrode with some tissue remnants. (d) High magnification Pt-Ir coated electrode showing a region of exposed Pt base metal (×). (e) Extent of coating coverage on Pt-Ir electrodes. Effect of charge density on (f) charge storage capacity, (g) charge injection limit, and (h) voltage transient impedance. Mean Pt data are dashed lines; mean Pt-Ir data are dotted lines. Charge density = 0 µC cm^{-2} phase for unstimulated electrodes, ~10 μC cm^{-2} phase for flanking electrodes, ~20 μC cm^{-2} phase for centre electrodes. *$p \leq 0.05$; **$p \leq 0.01$; asterisks indicating significance are colour-coordinated by material.

Importantly, the Pt-Ir coated electrode arrays showed no adverse effects on AN density or neural thresholds compared to Pt electrodes, supporting the general biocompatible nature of the Pt-Ir coating.

4.3. Adhesion of Pt-Ir coating on the electrode surface

Although a major issue associated with conductive coatings has been the extensive delamination observed following chronic *in vivo* implantation [28, 54], we have previously reported that electroplated Pt-Ir was a mechanically stable coating evaluated using an *in vitro* adhesion test [33]. In the present study we observed small regions without Pt-Ir on the surface of the majority of Pt-Ir electrodes; however, because there were small regions devoid of Pt-Ir observed directly after coating (figure 7(e)) and no SEM images were taken prior to implantation (figure 1(a)), it is unclear whether any of these regions appeared during the course of the implantation period or were all present before

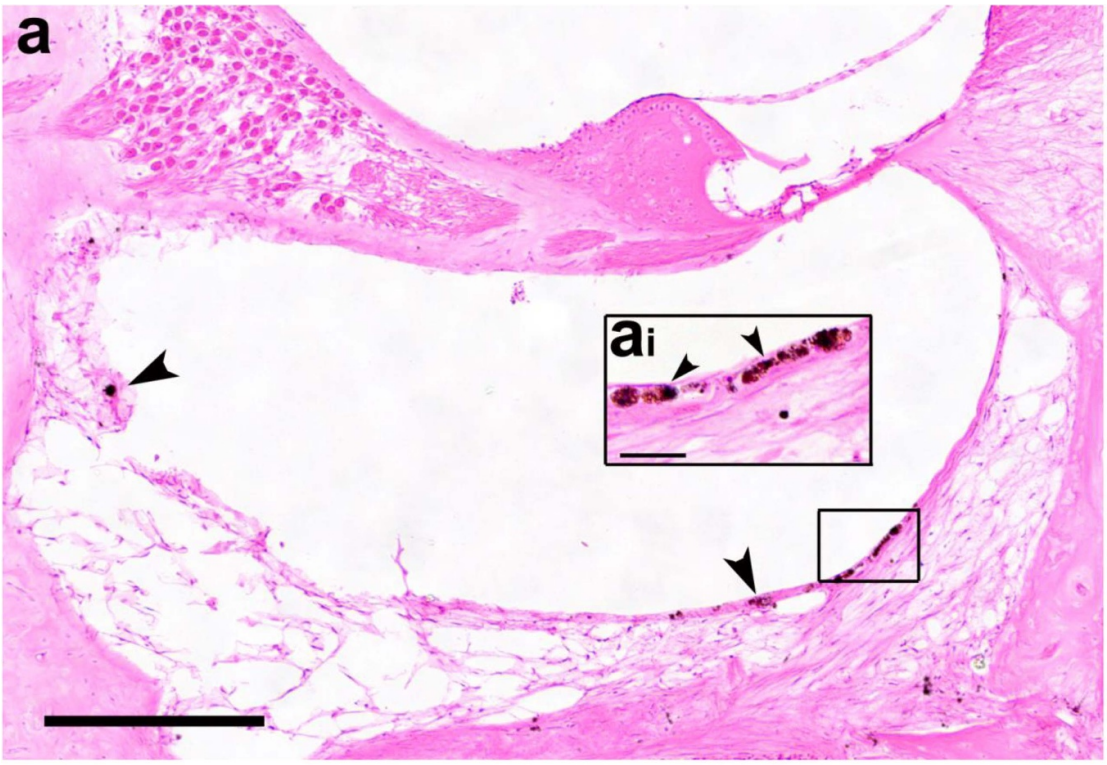

Figure 8. (a) Photomicrograph of the lower basal turn of chronically implanted and stimulated cochlea from PtIr05. Particulate material localized to the electrode tissue capsule (arrowhead). Scale bar = 200 μm. (ai) Inset illustrates higher magnification of a region of the tissue capsule with sub-micron particles that have been phagocytosed by cells lining the tissue capsule. Scale bar = 25 μm.

implantation. Regardless, the extent of Pt-Ir non-coverage was small and unrelated to the extent of electrical stimulation and was not correlated with electrochemical performance.

Particulate Pt-Ir was identified in the majority of cochleae implanted with Pt-Ir coated electrodes. These particles were incorporated into the tissue capsule, with sub-micron particles undergoing phagocytosis. These histological observations indicate that the particulate Pt-Ir was introduced into the cochlea during, or shortly after, the insertion of the electrode array rather than in the course of its removal on completion of the stimulation program. The amount of Pt-Ir in the tissue was not quantified; therefore, a correlation between the amount of Pt-Ir in the tissues and the coverage of Pt-Ir seen under SEM (figure 7(e)) was not established.

There are a number of potential sources for the origin of Pt-Ir particles within the cochlea: (i) Pt-Ir particles were released from the coating during the insertion of the array; (ii) Pt-Ir particles on the silicone carrier proximal to the electrodes dislodged during insertion; and/or (iii) traces of silicone that remained on the electrode surface following manufacturing contained Pt-Ir particles and this material was removed during the insertion [55]. Given that there was evidence of loss of Pt-Ir particles in the tissue and we did not observe silicone within the implanted cochlea, it is most likely some Pt-Ir particles were removed from cochlear implant during electrode insertion. We note that the aperture of the round window, the entry site for the electrode array, is narrow in the rat; it is possible that the surface of the electrode array contacted the bony rim of the round window during insertion of the array. If this observation is correct, it would be possible to enlarge the opening into the cochlea during surgery. Alternatively, the Pt-Ir coating could be temporarily protected using a biodegradable film such as gelatin that is applied to the electrode array prior to insertion [56].

Finally, recent studies have demonstrated evidence of Pt particulates in the cochleae following long-term use of commercially available cochlear implants [57–60]. While not desirable, we recently showed no evidence of neural loss or impaired neural function in cochleae exhibiting particulate Pt as a result of electrode corrosion [38].

Overall the Pt-Ir coating evaluated in the present study performed well *in vivo*. Although the electrochemical performance was variable, the coating did not evoke an adverse tissue response or a reduction in neural function. Moreover, Pt-Ir coatings have potential application in other neural prostheses such as retinal prostheses [61], deep brain stimulation [62] and intraspinal microstimulation [63].

5. Conclusion

Chronic implantation and electrical stimulation of electrodeposited Pt-Ir coated electrodes in rat cochleae demonstrated significant increases in CSC and CIL and significant decreases in impedance in benchtop testing before and on completion of the stimulation program compared to uncoated Pt electrodes. *In vivo,* CSC and CIL of Pt-Ir electrodes remained significantly higher than Pt electrodes. VT impedance (the sum of the access resistance and polarization impedance) for Pt-Ir electrodes was significantly lower than Pt during the first few days of stimulation but increased over the 5 week implantation period. The increase in VT impedance can be accounted for with an increase in tissue resistance, which was similar for both coated and uncoated electrodes. The similar increase in tissue resistance is consistent with the comparable tissue responses seen in the histology, which showed that Pt and Pt-Ir coated electrodes evoked a mild tissue response that typically consisted of mature fibroblasts. Furthermore, there was no evidence of increased neural loss or loss of neural function in cochleae implanted with Pt-Ir electrodes, even though a small number of Pt-Ir particles were evident in histological sections. While further research to reduce the release of Pt-Ir particles into the tissue during implantation is desirable, electrodeposited Pt-Ir shows promise as an improved electrode coating material for use in active neural prostheses.

Acknowledgments

This work was funded by the NHMRC of the Australian Government (APP1122055) and the Garnett Passe and Rodney Williams Memorial Foundation for which we are most grateful. The Bionics Institute acknowledges support of the Victorian Government through Operational Infrastructure Support Program. We thank Drs A Thompson and T Hyakumara, C McGowan, and R Thomas and the electrode fabrication team from the Bionics Institute; the staff of EMSU, St Vincent's Hospital Melbourne for animal care; and R Curtain and the SEM Facility at Bio21, University of Melbourne for their technical assistance. Platinum Group Coatings (PGC) acknowledges the support of the Pasadena Bioscience Collaborative and thanks to J Sharkey for preparing test samples.

Conflicts of Interest:

Curtis Lee, Greg Weiland, Artin Petrossians, John Whalen are employed by Platinum Group Coatings (PGC), which provided the electrodeposited Pt-Ir coatings. Artin Petrossians and John Whalen are also part owners of PGC. The remaining authors declare no conflicts of interest.

ORCID iDs

Ashley N Dalrymple https://orcid.org/0000-0001-8566-7178
Mario Huynh https://orcid.org/0000-0002-5780-1891
Bryony A Nayagam https://orcid.org/0000-0003-1069-6059
Curtis D Lee https://orcid.org/0000-0001-8295-7786
Greg R Weiland https://orcid.org/0000-0001-9213-3609
Artin Petrossians https://orcid.org/0000-0003-2967-8205
John J https://orcid.org/0000-0002-5202-4747
James B Fallon https://orcid.org/0000-0003-2686-3886
Robert K Shepherd https://orcid.org/0000-0002-4239-3362

References

[1] Clark G M 2003 *Cochlear Implants: Fundamentals and Applications* (New York: Springer)
[2] Shepherd R K, Hatsushika S and Clark G M 1993 Electrical stimulation of the auditory nerve: the effect of electrode position on neural excitation *Hear. Res.* **66** 108–20
[3] Roche J P and Hansen M R 2015 On the Horizon: cochlear Implant Technology *Otolaryngol. Clin. North Am.* **48** 1097–116
[4] Shepherd R K, Franz B K H G and Clark G M 1990 The biocompatibility and safety of cochlear prostheses ed G Clark, Y C Tong and J F Patrick *Cochlear Prostheses* (New York: Churchill Livingstone) pp 69–98
[5] Stover T and Lenarz T 2009 Biomaterials in cochlear implants *GMS Curr. Top. Otorhinolaryngol Head Neck Surg.* **8** 10
[6] Cogan S F 2008 Neural stimulation and recording electrodes *Annu. Rev. Biomed. Eng.* **10** 275–309
[7] Fu Q J and Nogaki G 2005 Noise susceptibility of cochlear implant users: the role of spectral resolution and smearing *J. Assoc. Res. Otolaryngol.* **6** 19–27
[8] Sucher C M and McDermott H J 2007 Pitch ranking of complex tones by normally hearing subjects and cochlear implant users *Hear. Res.* **230** 80–87
[9] Boex C, de Balthasar C, Kos M I and Pelizzone M 2003 Electrical field interactions in different cochlear implant systems *J. Acoust. Soc. Am.* **114** 2049–57
[10] Snyder R L, Middlebrooks J C and Bonham B H 2008 Cochlear implant electrode configuration effects on activation threshold and tonotopic selectivity *Hear. Res.* **235** 23–38
[11] George S S, Wise A K, Fallon J B and Shepherd R K 2015 Evaluation of focused multipolar stimulation for cochlear implants in long-term deafened cats *J. Neural Eng.* **12** 036003
[12] Bierer J A, Bierer S M and Middlebrooks J C 2010 Partial tripolar cochlear implant stimulation: spread of excitation and forward masking in the inferior colliculus *Hear. Res.* **270** 134–42
[13] Noble J H, Labadie R F, Gifford R H and Dawant B M 2013 Image-guidance enables new methods for customizing cochlear implant stimulation strategies *IEEE Trans. Neural Syst. Rehabil. Eng.* **21** 820–9
[14] Ludwig K A, Uram J D, Yang J, Martin D C and Kipke D R 2006 Chronic neural recordings using silicon microelectrode arrays electrochemically deposited with a poly(3,4-ethylenedioxythiophene) (PEDOT) film *J. Neural Eng.* **3** 59–70

[15] Venkatraman S, Hendricks J, King Z A, Sereno A J, Richardson-Burns S, Martin D and Carmena J M 2011 *In vitro* and *in vivo* evaluation of PEDOT microelectrodes for neural stimulation and recording *IEEE Trans. Neural Syst. Rehabil. Eng.* A **19** 307–16
[16] Alba N A, Du Z J, Catt K A, Kozai T D and Cui X T 2015 *In vivo* electrochemical analysis of a PEDOT/MWCNT neural electrode coating *Biosensors* **5** 618–46
[17] Cui X T and Zhou D D 2007 Poly (3,4-ethylenedioxythiophene) for chronic neural stimulation *IEEE Trans. Neural Syst. Rehabil. Eng.* A **15** 502–8
[18] Green R A, Matteucci P B, Hassarati R T, Giraud B, Dodds C W, Chen S, Byrnes-Preston P J, Suaning G J, Poole-Warren L A and Lovell N H 2013 Performance of conducting polymer electrodes for stimulating neuroprosthetics *J. Neural Eng.* **10** 016009
[19] Kolarcik C L, Catt K, Rost E, Albrecht I N, Bourbeau D, Du Z, Kozai T D Y, Luo X, Weber D J and Tracy Cui X 2015 Evaluation of poly(3,4-ethylenedioxythiophene)/carbon nanotube neural electrode coatings for stimulation in the dorsal root ganglion *J. Neural Eng.* **12** 016008
[20] Goding J, Gilmour A, Martens P, Poole-Warren L and Green R 2017 Interpenetrating conducting hydrogel materials for neural interfacing electrodes *Adv. Healthc. Mater.* **6** 10
[21] Chikar J A, Hendricks J L, Richardson-Burns S M, Raphael Y, Pfingst B E and Martin D C 2012 The use of a dual PEDOT and RGD-functionalized alginate hydrogel coating to provide sustained drug delivery and improved cochlear implant function *Biomaterials* **33** 1982–90
[22] Hassarati R T, Dueck W F, Tasche C, Carter P M, Poole-Warren L A and Green R A 2014 Improving cochlear implant properties through conductive hydrogel coatings *IEEE Trans. Neural Syst. Rehabil. Eng.* A **22** 411–8
[23] Negi S, Bhandari R, Rieth L and Solzbacher F 2010 In vitro comparison of sputtered iridium oxide and platinum-coated neural implantable microelectrode arrays *Biomed. Mater.* **5** 15007
[24] Negi S, Bhandari R, Rieth L, Van Wagenen R and Solzbacher F 2010 Neural electrode degradation from continuous electrical stimulation: comparison of sputtered and activated iridium oxide *J. Neurosci. Methods* **186** 8–17
[25] Angelov S D, Koenen S, Jakobi J, Heissler H E, Alam M, Schwabe K, Barcikowski S and Krauss J K 2016 Electrophoretic deposition of ligand-free platinum nanoparticles on neural electrodes affects their impedance in vitro and in vivo with no negative effect on reactive gliosis *J. Nanobiotechnol.* **14** 3
[26] Meyer R D, Cogan S F, Nguyen T H and Rauh R D 2001 Electrodeposited iridium oxide for neural stimulation and recording electrodes *IEEE Trans. Neural Syst. Rehabil. Eng.* **9** 2–11
[27] Green R A, Lovell N H, Wallace G G and Poole-Warren L A 2008 Conducting polymers for neural interfaces: challenges in developing an effective long-term implant *Biomaterials* **29** 3393–9
[28] Boehler C, Oberueber F, Schlabach S, Stieglitz T and Asplund M 2017 Long-term stable adhesion for conducting polymers in biomedical applications: irox and nanostructured platinum solve the chronic challenge *ACS Appl. Mater. Interfaces* **9** 189–97
[29] Green R A, Hassarati R T, Bouchinet L, Lee C S, Cheong G L, Yu J F, Dodds C W, Suaning G J, Poole-Warren L A and Lovell N H 2012 Substrate dependent stability of conducting polymer coatings on medical electrodes *Biomaterials* **33** 5875–86
[30] Tykocinski M, Duan Y, Tabor B and Cowan R S 2001 Chronic electrical stimulation of the auditory nerve using high surface area (HiQ) platinum electrodes *Hear. Res.* **159** 53–68
[31] Petrossians A, Whalen J J, Weiland J D and Mansfeld F 2011 Electrodeposition and characterization of thin-film platinum-iridium alloys for biological interfaces *J. Electrochem. Soc.* **158** D269–D276
[32] Lee C D, Hudak E M, Whalen J J, Petrossians A and Weiland J D 2018 Low-impedance, high surface area Pt-Ir electrodeposited on cochlear implant electrodes *J. Electrochem. Soc.* **165** G3015–G3017
[33] Dalrymple A N *et al* 2019 Electrochemical and mechanical performance of reduced graphene oxide, conductive hydrogel, and electrodeposited Pt-Ir coated electrodes: an active in vitro study *J. Neural Eng.* **17** 016015
[34] Cassar I R, Yu C, Sambangi J, Lee C D, Whalen J J III, Petrossians A and Grill W M 2019 Electrodeposited platinum-iridium coating improves in vivo recording performance of chronically implanted microelectrode arrays *Biomaterials* **205** 120–32
[35] Lu W, Xu J and Shepherd R K 2005 Cochlear implantation in rats: a new surgical approach *Hear. Res.* **205** 115–22
[36] Petrossians A, Whalen J J, Weiland J D and Mansfeld F 2011 Surface modification of neural stimulating/recording electrodes with high surface area platinum-iridium alloy coatings *Ann. Int. Conf. IEEE Eng. Med. Biol. Soc.* pp 3001–4
[37] Leung R T, Shivdasani M N, Nayagam D A and Shepherd R K 2015 In vivo and in vitro comparison of the charge injection capacity of platinum macroelectrodes *IEEE Trans. Biomed. Eng.* **62** 849–57
[38] Shepherd R K, Carter P, Enke Y L, Wise A K and Fallon J B 2019 Chronic intracochlear electrical stimulation at high charge densities results in platinum dissolution but not neural loss or functional changes in vivo *J. Neural Eng.* **16** 026009
[39] Senn P 2015 Neurostimulation for the management of pain *PhD Medical Bionics* (Melbourne: University of Melbourne)
[40] Patrick J F, SeIigman P M, Money D K and Kuzma J A 1990 Engineering *Cochlear Prostheses*, ed G M Clark, Y C Tong and J F Patrick (Edinburgh: Churchill Livingston) pp 99–124
[41] George S S, Shivdasani M N, Wise A K, Shepherd R K and Fallon J B 2015 Electrophysiological channel interactions using focused multipolar stimulation for cochlear implants *J. Neural Eng.* **12** 066005
[42] Schneider C A, Rasband W S and Eliceiri K W 2012 NIH Image to ImageJ: 25 years of image analysis *Nat. Methods* **9** 671–5
[43] Wise A K, Tan J, Wang Y, Caruso F and Shepherd R K 2016 Improved auditory nerve survival with nanoengineered supraparticles for neurotrophin delivery into the deafened cochlea *PLoS ONE* **11** e0164867
[44] Dalrymple A N, Aregueta Robles U, Huynh M, Nayagam B A, Green R A, Poole-Warren L A, Fallon J B and Shepherd R K 2020 Electrochemical and biological performance of chronically stimulated conductive hydrogel electrodes *J. Neural Eng.* **17** 026018
[45] Xu J, Shepherd R K, Millard R E and Clark G M 1997 Chronic electrical stimulation of the auditory nerve at high stimulus rates: a physiological and histopathological study *Hear. Res.* **105** 1–29
[46] Tykocinski M, Cohen L T and Cowan R S 2005 Measurement and analysis of access resistance and polarization impedance in cochlear implant recipients *Otology Neurotology* **26** 948–56
[47] Williams J C, Hippensteel J A, Dilgen J, Shain W and Kipke D R 2007 Complex impedance spectroscopy for monitoring tissue responses to inserted neural implants *J. Neural Eng.* **4** 410–23
[48] Vara H and Collazos-Castro J E 2019 Enhanced spinal cord microstimulation using conducting polymer-coated carbon microfibers *Acta Biomater.* **90** 71–86
[49] Fujikado T *et al* 2007 Evaluation of phosphenes elicited by extraocular stimulation in normals and by suprachoroidal-transretinal stimulation in patients with retinitis pigmentosa *Graefe's Arch. Clinical Exp. Ophthalmol.* **245** 1411–9
[50] Pfingst B E, Bowling S A, Colesa D J, Garadat S N, Raphael Y, Shibata S B, Strahl S B, Su G L and Zhou N 2011 Cochlear infrastructure for electrical hearing *Hear. Res.* **281** 65–73

[51] Beebe X and Rose T L 1988 Charge injection limits of activated iridium oxide electrodes with 0.2 msec pulses in bicarbonate buffered saline *IEEE Trans. Biomed. Eng.* **BME-35** 494–5
[52] Shibata S B, Budenz C L, Bowling S A, Pfingst B E and Raphael Y 2011 Nerve maintenance and regeneration in the damaged cochlea *Hear. Res.* **281** 56–64
[53] Laube T, Schanze T, Brockmann C, Bolle I, Stieglitz T and Bornfeld N 2003 Chronically implanted epidural electrodes in Gottinger minipigs allow function tests of epiretinal implants *Graefe's Arch. Clinical Exp. Ophthalmol.* **241** 1013–9
[54] Salatino J W, Ludwig K A, Kozai T D and Purcell E K 2017 Glial responses to implanted electrodes in the brain *Nat. Biomed. Eng.* **1** 862–77
[55] Armstrong S 2019 Investigation of platinum electrode degradation in bovine calf serum *BE (Hons)* School of Materials Science and Engineering UNSW, Sydney
[56] Kohler P, Wolff A, Ejserholm F, Wallman L, Schouenborg J and Linsmeier C E 2015 Influence of probe flexibility and gelatin embedding on neuronal density and glial responses to brain implants *PLoS ONE* **10** e0119340
[57] O'Malley J T, Burgess B J, Galler D and Nadol J B Jr. 2017 Foreign body response to silicone in cochlear implant electrodes in the human *Otology Neurotology* **38** 970–7
[58] Nadol J B Jr , O'Malley J T, Burgess B J and Galler D 2014 Cellular immunologic responses to cochlear implantation in the human *Hear. Res.* **318** 11–17
[59] Spiers K, Cardamone T, Furness J B, Clark J C M, Patrick J F and Clark G M 2016 An X-ray fluorescence microscopic analysis of the tissue surrounding the multi-channel cochlear implant electrode array *Cochlear Implants Int.* **17** 129–31
[60] Clark G M *et al* 2014 Biomedical studies on temporal bones of the first multi-channel cochlear implant patient at the university of Melbourne *Cochlear Implants Int.* **10** S1–S15
[61] Halpern M E and Fallon J 2010 Current waveforms for neural stimulation-charge delivery with reduced maximum electrode voltage *IEEE Trans. Biomed. Eng.* **57** 2304–12
[62] Ramirez-Zamora A *et al* 2017 Evolving applications, technological challenges and future opportunities in neuromodulation: proceedings of the fifth annual deep brain stimulation think tank *Front. Neurosci.* **11** 734
[63] Dalrymple A N, Everaert D G, Hu D S and Mushahwar V K 2018 A speed-adaptive intraspinal microstimulation controller to restore weight-bearing stepping in a spinal cord hemisection model *J. Neural. Eng.* **15** 056023